scientific data

Check for updates

OPEN

DATA DESCRIPTOR

Chemical Profiles of Particulate Matter Emitted from Anthropogenic Sources in Selected Regions of China

Lixin Zheng[1], Di Wu[1] ✉, Xiu Chen[1], Yang Li[1], Anyuan Cheng[1], Jinrun Yi[1] & Qing Li[1,2] ✉

Particulate matter (PM) emissions from anthropogenic sources contribute substantially to air pollution. The unequal adverse health effects caused by source-emitted PM emphasize the need to consider the discrepancy of PM-bound chemicals rather than solely focusing on the mass concentration of PM when making air pollution control strategies. Here, we present a dataset about chemical compositions of real-world PM emissions from typical anthropogenic sources in China, including industrial (power, industrial boiler, iron & steel, cement, and other industrial process), residential (coal/biomass burning, and cooking), and transportation sectors (on-road vehicle, ship, and non-exhaust emission). The data was obtained under the same strict quality control condition on field measurements and chemical analysis, minimizing the uncertainty caused by different study approaches. The concentrations of PM-bound chemical components, including toxic elements and PAHs, exhibit substantial discrepancies among different emission sectors. This dataset provides experimental data with informative inputs to emission inventories, air quality simulation models, and health risk estimation. The obtained results can gain insight into understanding on source-specific PMs and tailoring effective control strategies.

Background & Summary

Particulate matter (PM) emitted from various anthropogenic sources has been identified as the key constituent resulting in ambient air pollution and further causing adverse effects on human health and climate change[1–5]. The mass concentration of ambient PMs, generally linked with exposure risk on disease burden assessments[6–8], is a routine parameter of air quality monitoring and control guidelines worldwide, which implicitly based on the assumption that PMs are the same among regions. Since PMs in the atmosphere is a cocktail of complex chemicals, including elements (such as trace elements, transition metals, and crustal elements), water-soluble inorganic ions, and carbonaceous species[9,10], more concern should be paid to the chemical compositions of PMs which may trigger different toxic endpoints and health effects[11–13], when evaluating PM exposure risks.

The components of source-specific PMs show a great discrepancy in the relative content of chemicals for individual source, mainly attributing to the heterogeneity in applicating fuel types, production raw materials, industrial processes, and air pollution control technologies[14–17]. Due to the lack of experimental data from local emission sources, early air pollution emission inventories in China had been mainly developed by using bottom-up methodology with activity rates and emission factors adopted from developed countries[18]. The heterogeneity of source-specific PMs between China and other countries could result in great uncertainty when using those non-local chemical profiles. Therefore, the study of updated and comprehensive chemical profiles of individual source-specific PMs across local regions in China, especially including those components with adverse health and environment effects, is necessary and meaningful to better evaluate their potential impacts.

With increasingly abundant simulation experiments and field measurements[19–29], several air pollution emission inventories, such as the Peking University's emission inventory, the air benefit and cost and attainment assessment system (ABaCAS) inventory, and the Multi-resolution Emission Inventory for China (MEIC), have

[1]Department of Environmental Science and Engineering, Shanghai Key Laboratory of Atmospheric Particle Pollution and Prevention, Fudan University, Shanghai, 200433, China. [2]Shanghai Institute of Eco-Chongming (SIEC), 20 Cuiniao Road, Chenjia Town, Chongming District, Shanghai, 202162, China. ✉e-mail: di_wu@fudan.edu.cn; qli@fudan.edu.cn

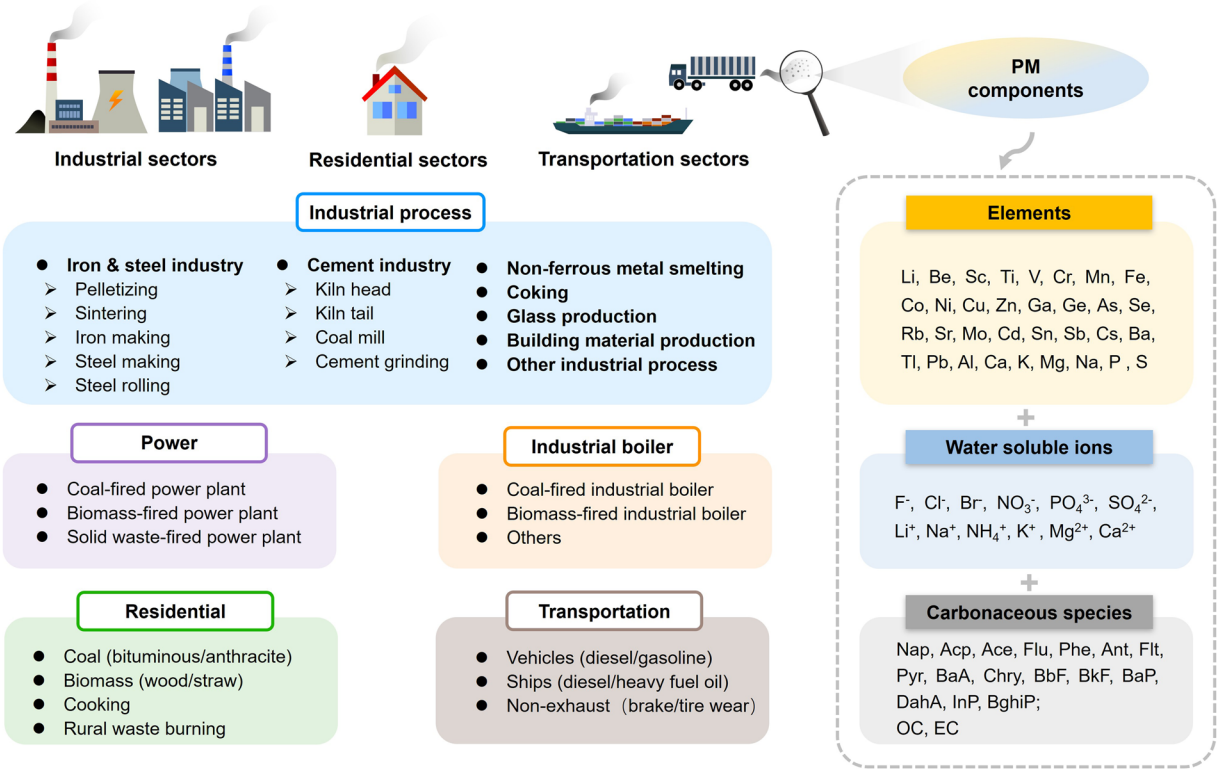

Fig. 1 Framework of the dataset about chemical compositions of PM emitted from typical anthropogenic sources. Emission sources are classified into industrial sectors (including power industry, industrial boilers, and industrial process), residential sectors (including coal/biomass burning, cooking emission, and rural solid waste burning), and transportation sectors (including tailpipe exhaust of vehicles /ships, and non-exhaust of vehicles). PM components include elements (i.e., Li, Be, Sc, Ti, V, Cr, Mn, Fe, Co, Ni, Cu, Zn, Ga, Ge, As, Se, Rb, Sr, Mo, Cd, Sn, Sb, Cs, Ba, Tl, Pb, Al, Ca, K, Mg, Na, P, and S), water-soluble ions (i.e., F^-, Cl^-, Br^-, NO_3^-, PO_4^{3-}, SO_4^{2-}, Li^+, Na^+, NH_4^+, K^+, Mg^{2+}, and Ca^{2+}), OC/EC, and 16 US EPA priority PAHs (Nap, Acp, Ace, Flu, Phe, Ant, Flt, Pyr, BaA, Chry, BbF, BkF, BaP, DahA, InP, and BghiP).

been developed in China within the past two decades[30–36]. These studies have strengthened our understanding of the PM emissions into the atmosphere and provided data for policy-making to control air pollution in China. However, the available data on PM-bound chemicals mainly focused on limited species of chemicals or source categories. In addition, the non-uniform methods of PM sample sampling, chemical analysis, simulation condition, and rough emission source categories without considering specific subcategories resulted in a large uncertainty and further influenced the accurate quantification of source contributions to atmospheric PMs[23,37,38]. Industrial sectors contributed the majority of China's anthropogenic PM emissions. In addition, residential and transportation sectors also contributed a lot to PM emissions considering China's large population of rural and urban residents[30,39–41]. To better evaluate the PM effects, it is crucial to have a comprehensive understanding of the chemical characteristics of source-specific PM in China. Although existence of many well-studied topics focusing on emission characteristics of certain PM-bound chemical species[23,24,42], a systematical dataset containing simultaneously concerned inorganic and organic components in PMs based on field study in China is limited.

Here, an updated dataset about chemical components of PMs emitted from major anthropogenic sources based on field study in China is provided[43]. The emission sources, including typical industrial, residential, and transport sectors, can be roughly classified into 5 categories (i.e., power, industrial boiler, industrial process, residential, and transportation sectors) with more specific subcategories according to their applied fuel types, processes, and control technologies. The items of PM-bound components include elements (i.e., Li, Be, Sc, Ti, V, Cr, Mn, Fe, Co, Ni, Cu, Zn, Ga, Ge, As, Se, Rb, Sr, Mo, Cd, Sn, Sb, Cs, Ba, Tl, Pb, Al, Ca, K, Mg, Na, P, and S), water-soluble ions (i.e., F^-, Cl^-, Br^-, NO_3^-, PO_4^{3-}, SO_4^{2-}, Li^+, Na^+, NH_4^+, K^+, Mg^{2+}, and Ca^{2+}), organic carbon (OC), elemental carbon (EC), and 16 US Environmental Protection Agency (EPA) priority polycyclic aromatic hydrocarbons (PAHs), including naphthalene (Nap), acenaphthylene (Acp), acenaphthene (Ace), fluorene (Flu), phenanthrene (Phe), anthracene (Ant), fluoranthene (Flt), pyrene (Pyr), benzo[a]anthracene (BaA), chrysene (Chry), benzo[b]fluoranthene (BbF), benzo[k]fluoranthene (BkF), benzo[a]pyrene (BaP), benzo[g,h,i]perylene (BghiP), indeno[1,2,3-c,d]pyrene (InP), and dibenz[a,h]anthracene(DahA). Figure 1 illustrates the overview of this dataset[43], in which chemical components, such as toxic elements and PAHs, are concerned in priority. Water-soluble ions (WSIs), OC/EC, and other crustal elements are also recorded to present overall chemical profiles of source-specific PM. The study design and geographic distribution of field sampling sites is shown in Fig. 2.

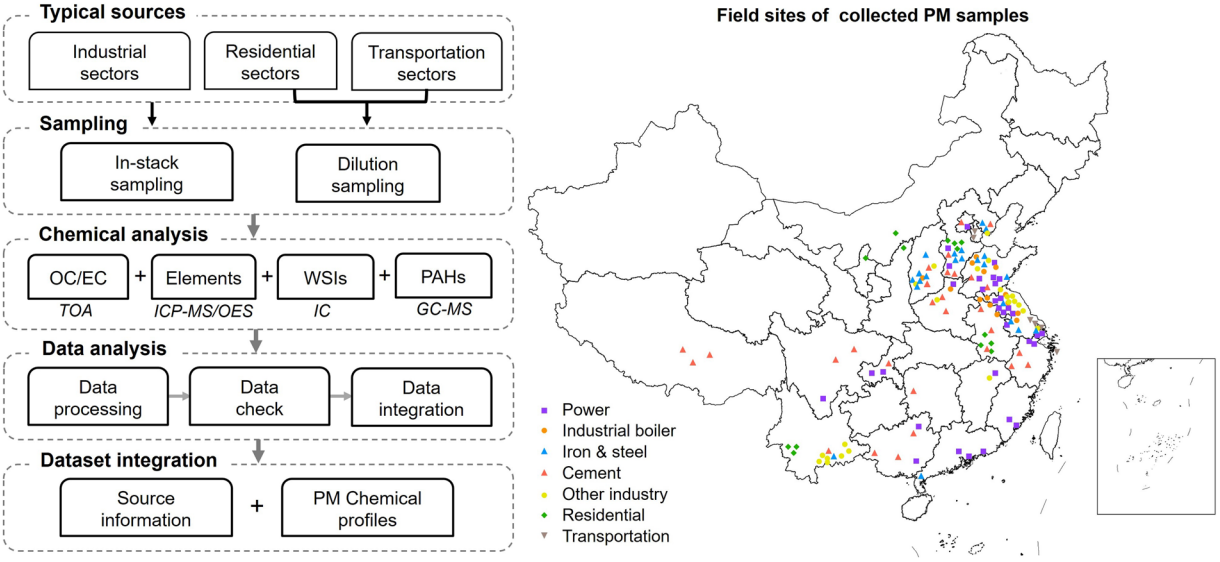

Fig. 2 Study design and spatial locations of field sites for PM emission source in mainland China. (**a**) The flow chart of dataset formation with main procedures, including field sampling from typical sources, chemical analysis, data analysis, and the final dataset integration. The instruments for chemical analysis are listed as follows: TOA indicates thermal/optical carbon analyser to test OC/EC. ICP-MS/ICP-OES means inductively coupled plasma mass spectrometer/optical emission spectrometry to detect elements. IC means ion chromatography to measure water-soluble ions. GC-MS means gas chromatograph mass spectrometer to test PAHs. (**b**) Geographic distribution of the field-studied industrial plants (including power, iron & steel, cement, and other industry), residential sites, and transportation sites.

The source-specific PM profiles could be integrated into source apportionment and emission inventory study, as well as serve as basic input data for multiple atmospheric chemistry transport models to further understand the potential effects resulting from ambient PMs. The dataset provides local and comprehensive measurement data based on field study under the same quality control condition, decreasing the uncertainty induced by various study approaches. The basic data can be used for quantitative evaluations and spatial distributions of specific chemical components when conducting studies of PM emissions. This dataset can be also combined with PM emission inventories and atmospheric chemistry transport models, such as MEIC, ABaCAS emission inventories, and the Weather Research and Forecasting-Community Multiscale Air Quality (WRF-CMAQ) model, for further study. A comprehensive consideration of PM mass concentrations integrated with their multiple components would benefit the evaluation of adverse health effects contributed by individual PM emission sources. Further, the reuse of data would provide potential insights for transitioning air pollution control policies from mass-based approaches to health-oriented ones.

Methods

Field measurements. *Field sampling of PM emission from industrial sectors.* The field measurements of 135 typical units in industry sources were conducted across mainland China from 2017 to 2022. The observed industry sources involve emission-intensive sectors (including power plants, iron & steel plants, and cement plants) and other industry sources (including non-ferrous metal smelting plants, coking plants, glass production plants, building material production plants, and other industrial processes). The power sectors involve 35 units including coal-fired power plants (CFPPs), biomass-fired power plants (BFPPs), and municipal solid waste-fired power plants (WFPPs). The electricity generation capacities of the tested units ranged from 12 MW to 1000 MW. The CFPPs of this study mainly use bituminous coals as fuel and employed either pulverized coal boilers or circulating fluidized bed boilers. The iron and steel sectors, with a total of 72 samples, include 22 typical units covering the major production processes of pig iron and crude steel, such as pelletizing, sintering, ironmaking, steelmaking, and steel rolling. The cement sectors involve 29 production units equipped with new dry process production lines with production capacity ranging from 2000 to 12000 t/d. All the cement production units utilized precalciner kilns, a dominant kiln type in China. The other industry sources include 18 plants that use industrial boilers, 10 units of non-ferrous metal smelting plants, 6 units of coking plants, 10 units/production lines of glass plants, and 5 other industrial processes. Each tested industrial unit was equipped with air pollution control devices (APCDs), which include combinations of the dedusting system (e.g., electrostatic precipitator, fabric filter) for PM reduction, de-NO_x system (e.g., selective noncatalytic reduction, selective catalytic reduction) for NO_x reduction, and flue gas desulfurization system (e.g., wet flue gas desulfurization, semidry flue gas desulfurization) for SO_2 reduction.

An isokinetic sampling system (C-5000, ESC, USA) was employed to collect PM samples from industrial flue gases according to US EPA Methods 17 and 201A[15,44,45]. This widely-used sampling system for collecting PM

samples from stationary sources mainly consists of a heated stainless steel sampling probe with nozzle/cyclone sets, a 47 mm filter holder, a set of glassware, and a console with a vacuum pump. The isokinetic sampling nozzle and probe, and the stainless-steel filter holder were heated and maintained at 120°C throughout the entire sampling process to avoid condensation of water vapor and flue gas. PM samples were collected on quartz fiber filters (QFFs, Whatman 1851-865, UK) and Teflon filters (TFs, Whatman 7592-104, UK) for subsequent analysis. The sampling duration for each industrial unit ranged from 30 to 120 min. Three successful samplings in parallel of the selected industrial units/sites were conducted. Additionally, field-blank filters were also collected to subtract the background concentrations of each pollutant. The PM samples were stored at −20°C before further weighing and analysis. Meanwhile, some industrial flue gas dust samples were also collected from dedust systems near the end-pipe. Additional information regarding the field sampling techniques and quality control methods for industrial sectors can be found in our previous studies[15,44,46].

Field sampling of PM emissions from residential sectors. Field measurements of residential solid fuel burning for heating and cooking were conducted in typical households in rural areas in China, which included the main types of commonly used solid fuels (i.e., bituminous coal, anthracite coal, wood and, crop residue) and stoves (i.e., brick stove, three-stone stove, iron stove, and gasifier stove). The stoves used in this study remained in their usual locations of household, while the chimneys were replaced with shorter sections to hold their outlets under an exhaust hood equipped with an electric blower as a constant-volume flue gas dilution system. Water heating, which intentionally limited the maximum temperature of the water to 80°C, was used as the field test method to avoid interference of smoke emissions or additional vapor from cooking activity. Coal samples were ignited with pine chips until a stable flame was observed, while biomass samples were ignited with lighters. The whole burning cycle lasted about 2–8 h for coal, 20–40 min for wood, and 15–30 min for biomass, respectively. The diluted flue gases passed through a vent pipe with a fixed flow rate of 22 m^3/min. A homemade sampler was used to collect total suspended particulate (TSP) samples, and a $PM_{2.5}$ cyclone (URG 2000-30EH, USA) was used to collect $PM_{2.5}$ samples. Two parallel PM samples were collected on QFFs (Whatman 1851-865, UK) and TFs (Whatman 7592-104, UK) for different analyses.

Field measurements of PM emissions from cooking were conducted in a canteen, serving barbecue and Chinese-style dishes. End-pipe emissions of the ventilation system on the roof covering the whole cooking process, and three individual cooking styles (i.e., barbecuing, stir-frying, and deep-frying), were chosen as representative cooking emission conditions. The $PM_{2.5}$ samples from end-pipe emissions were collected on the 210 mm × 297 mm QFFs (Whatman 1851-865, UK) using a high-volume air sampler (HV-R500, Sibata, Japan) at a flow rate of 1100 L/min. PM emissions from three individual cooking styles were sampled with a flow rate of 16.7 L/min. A $PM_{2.5}$ cyclone (2000-30EH, URG, USA), positioned near the range hood above the cooking workspace at a temperature similar to the ambient environment, was used to collect samples on QFFs (Whatman 1851-865, UK). The PM samples collection covers one complete cooking process and was repeated at least twice. The additional information on field sampling set and quality control methods of household solid fuel burning and cooking emission can be found in our previous studies[11,47–49].

Field sampling of PM emissions from transportation sectors. The commonly used on-road light-duty gasoline vehicles (LDGVs) and heavy-duty diesel vehicles (HDDVs) in China were selected for field measurements of tailpipe exhausts. A total of 10 LDGVs were chosen, which represent major types of LDGVs in China, to perform field measurements on an electric chassis dynamometer (VULCAN EMSCD48, Horiba, Japan) to simulate real-world driving conditions. The engine displacements ranged from 1.5 to 2.3 L. Measurements were conducted with the Worldwide harmonized Light vehicles Test Cycle (WLTC) under hot engine start conditions. Six typical HDDVs were tested on a chassis dynamometer (ECDM-72H Maha, Germany). The engine displacements ranged from 6.5 to 9.7 L. Each HDDV was tested through the Chinese World Transient Vehicle cycle (C-WTVC). Tailpipe emissions were diluted with clean air using a constant volume sampling (CVS) system (CVS-7000, Horiba, Japan) with a fixed flow rate of 140 m^3/min in the CVS. A $PM_{2.5}$ cyclone (URG 2000-30EH) was used to collect $PM_{2.5}$ samples on both QFFs (Whatman 1851-865, UK) and TFs (Whatman 7592-104, UK).

In addition, 6 types of brake pads and 6 types of tires were selected to collect wear particles as representative non-exhaust emission samples of vehicles. Measurements of brake wear particles and tire particles were conducted on a brake dynamometer (Model 3000, LINK, USA) and a tire wear test system (ZF Friedrichshafen AG, Germany), respectively. They can simulate standard real-world driving conditions. The testing platforms were adapted to stay in chambers to minimize the influence of external ambient air. Filtered clean air can be drawn into the testing chambers, and wear PMs generated during system operation were sampled through a sampling tunnel. A $PM_{2.5}$ cyclone was used to collect $PM_{2.5}$ samples on both QFFs (Whatman 1851-865, UK) and TFs (Whatman 7592-104, UK).

Six types of commonly used ships including bulk cargo ships and container ships in China were selected for the field study. The gross tonnages of these tested ships varied between 495 and 1925, with the length ranging from 38 m to 67 m, and the width ranging from 7 to 15 m, respectively. Field measurements of ships were carried out in cruising mode with engine load being stable at about 80% of maximum power during the sampling period. A flue gas sampler (Dekati model 4000, Finland) equipped with an online dilution system was employed to dilute the vessel exhaust with a dilution ratio of 1:40. A homemade sampler and a $PM_{2.5}$ cyclone (URG 2000-30EH, USA) were used to collect TSP samples and $PM_{2.5}$ samples, respectively. The PM samples were collected on both QFFs (Whatman 1851-865, UK) and TFs (Whatman 7592-104, UK) for further analysis. Three successful samples were conducted for each test. The additional information on field sampling sets and quality control methods of transportation sectors can be found in our previous studies[13,16].

Chemical analysis. An inductively coupled plasma mass spectrometer (ICP-MS 7500a, Thermo, USA) was used to test the contents of trace elements (i.e., Li, Be, Sc, Ti, V, Cr, Mn, Fe, Co, Ni, Cu, Zn, Ga, Ge, As, Se, Rb, Sr, Mo, Cd, Sn, Sb, Cs, Ba, Tl, Pb), and another inductively coupled plasma optical emission spectrometry (ICP-OES, JarroU-Ash, USA) was used test other elements (i.e., Al, Ca, K, Mg, Na, P, and S). One-quarter of each filter was digested in Teflon tubes with 10 ml HNO_3 and 1 ml H_2O_2 using a microwave acid digestion system (MARS, CEM, USA). Heating procedure for microwave digestion was set holding 2 min at 120 °C, 5 min at 150 °C, and 45 min at 185 °C. The PM extract was filtered with 0.22 μm polytetrafluoroethylene (PTFE) syringe filters and subsequently was heated on a hot plate to mitigate the concentration of HNO_3 to 5%. Then the ultrapure water was added to dilute the PM extract to a volume of 10 mL.

The concentrations of WSIs in PM were determined by ion chromatography (940 Professional IC, Metrohm, Switzerland). One-quarter of each filter was extracted with 10 mL ultrapure water (Millipore, UK) and sonicated for 40 min at room temperature. The PM extract was filtered with 0.22 μm mixed cellulose esters (MCE) syringe filters. A C6-150/4.0 column (Metrohm, Switzerland) was employed to analyze cations (Li^+, Na^+, NH_4^+, K^+, Mg^{2+}, and Ca^{2+}) and a Supp 5-150/4.0 column (Metrohm, Switzerland) was employed to analyze anions (F^-, Cl^-, Br^-, NO_3^-, PO_4^{3-}, SO_4^{2-}).

A punched filter (0.508 cm^2) from quartz filter was used to determine carbonaceous species (including OC and EC). The OC/EC was determined by a thermal/optical carbon analyzer (DRI Model 2015, Magee, USA) with IMPROVE_A protocol. Eight temperature stages were designed to analyze OC fractions (at 140, 280, 480, and 580°C) and EC fractions (580, 740, and 840°C). More detailed information about instrument settings and test procedures can be found in our previous study or elsewhere[16,50].

A gas chromatograph coupled with a mass spectrometer (GC-MS 7890A-5975C, Agilent or ISQ 7000, Thermo Scientific, USA) was employed to detect US EPA 16 priority PAHs (i.e., Nap, Acp, Ace, Flu, Phe, Ant, Flt, Pyr, BaA, Chry, BbF, BkF, BaP, DahA, InP, and BghiP). One-quarter of each quartz fiber filter was extracted with dichloromethane/n-hexane (1:1, v/v) using an accelerated solvent extractor (ASE 350, Thermo Scientific, USA). The PM extracts were evaporated, purified, and finally concentrated to 1 mL before testing. More detailed information about instrument settings and test procedures can be found in our previous study[16,51]. The toxic equivalent benzo[a]pyrene values (BaP_{eq}) were quantified to estimate the carcinogenic potency of the targeted 16 PAHs. The toxic equivalency factors (TEFs) were employed to calculate PM-bound BaP_{eq} values according to the following equation.

$$BaP_{eq} = \sum_{i} C_i \cdot TEF_i,$$

where C_i means the concentration of each PAH, μg/g PM; TEF_i represents the toxic equivalency factor of individual PAH, which are obtained from previous study[52,53].

The TEFs for 16 PAHs have been widely used for estimating the health risks associated with PAH exposure[11,54–56]. The BaP_{eq} for a mixture of PM-bound PAHs reflects their overall toxicity levels. This estimation method also enables comparison with data from extensive literature, facilitating further analysis of the health risks associated with emission sources.

Data Records

The dataset is available at Figshare[43]. Two Excel files are provided in the dataset, including one named "Additional Description for the Dataset" and the other named "Mass Concentrations of PM-bound Chemicals Emitted from Typical Anthropogenic Sources in Selected Regions of China". The file named "Mass Concentrations of PM-bound Chemicals Emitted from Typical Anthropogenic Sources in Selected Regions of China" has five sheets exhibiting chemical profiles of PM emitted from individual sources (i.e., power, industrial boiler, industrial process, residential, and transportation) in this dataset. The concentration units for the elements, WSIs and OC/EC are presented in the form of mg/g PM, while the concentration units for PAHs are presented as μg/g. "N/A" means no available data. In addition, the descriptions of field sampling, including emission sources, locations of sampling sites, and other related information of sampling units (such as fuel types, products, production processes, and APCDs), are also provided in each sheet. The file named "Additional description for the dataset" involves a basic introduction about the category of emission sources, explanations for the abbreviation of APCDs, and concentration units of chemical components. The category of emission source in this dataset is modified according to ABaCAS emission inventory[57].

Technical Validation

Quality control procedure. In order to obtain reliable and valid data, we have implemented strict quality control procedures during the whole sampling and analysis processes, including field measurements, sample pretreatments, chemical composition measurements, detecting method validation, and data calculation. The major quality control procedures are described as follows.

The quartz filters were prebaked at 450 °C for 6 h to remove potential organic contaminants before usage. Blank filters (before sampling) and PM sample filters (after sampling) were all pre-stored for 24 h and weighed in a constant-temperature humidity chamber under the condition of 50% relative humidity and 20 °C. The filter holder was cleaned carefully every time before and after sampling. The sampling flow rate calibration and leakage check for the sampling system series were performed before each PM sampling. When making chemical components analysis, blank samples were also analyzed following the same procedure as the collected PM samples for blank correction. The correlation coefficients of standard calibration curves of target components are equal to or higher than 0.999. The method detection limits (MDLs) for target elements, water-soluble ions, and PAHs are 0.3–3.9 μg/L, 0.47–3.33 μg/L, and 23.9–51.2 μg/L, respectively. In addition, the recovery rates of target toxic elements and PAHs are about 83%–118%, and 80%–110%, respectively.

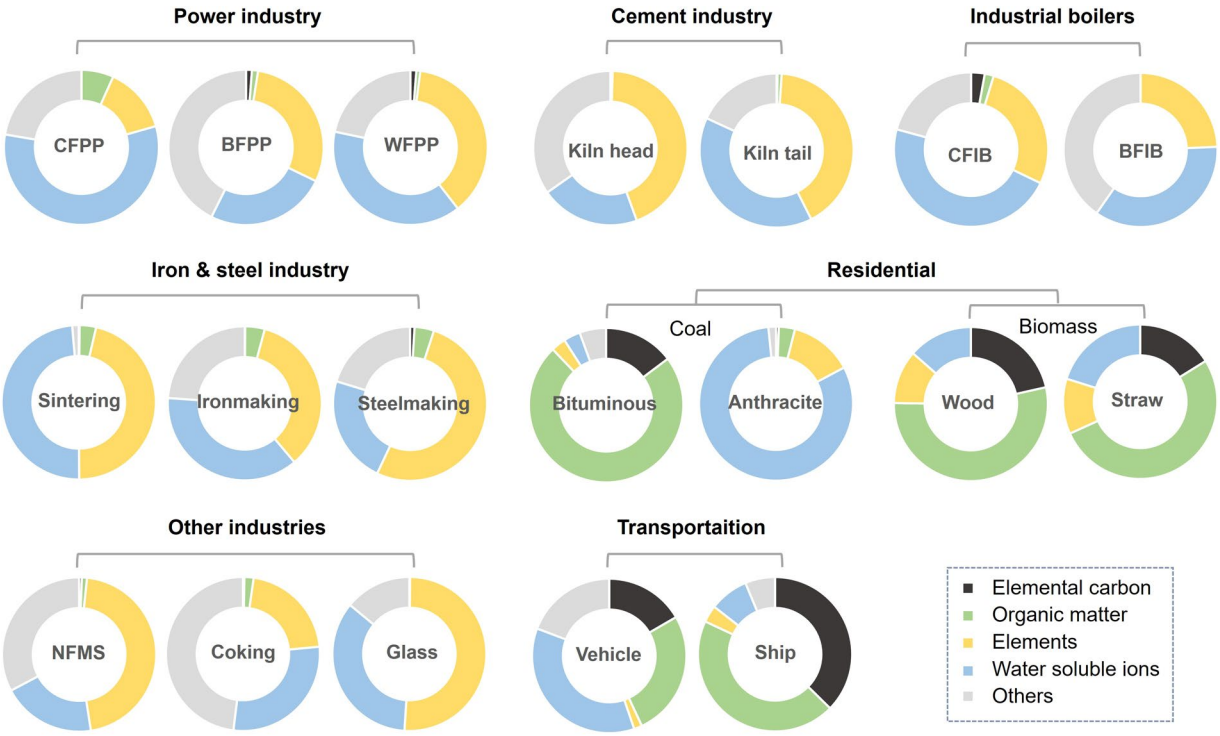

Fig. 3 Relative mass fractions of chemical components in PM emitted from typical anthropogenic sources. Doughnut Charts are grouped by sources and sub-grouped by fuel types or prevailing production processes. The content of organic matter is estimated as 1.2 times that of organic carbon. Others indicate undetermined species. CFPP: coal-fired power plants; BFPP: biomass-fired power plants; WFPP: solid waste-fired power plants; CFIB: coal-fired industrial boilers; BFIB: biomass-fired industrial boilers; NFMS: non-ferrous metal smelting. In addition, "Vehicle" and "Ship" refer to tailpipe exhaust in this figure.

Data summary. Here, we provide the data summary of this dataset, which doesn't fully cover all detailed processes in this descriptor. Taking the PM samples from the iron & steel industry for example, although the dataset actually covers pelletizing, sintering, ironmaking, steelmaking, rolling, and many other processes, only the three major processes, i.e., sintering, ironmaking, and steelmaking process, are included in the summary to make comparison with other sources and references in this descriptor.

The mass fractions of elements, WSIs, and carbonaceous species vary widely in tested PMs from different anthropogenic emission sources (Fig. 3). PMs emitted from industrial sectors have high proportions of elements (13.8-51.9%) and WSIs (19.6-57.1%), while PMs emitted from residential and transportation sources exhibit high proportions of organic matter (OM: 26.4-73.1%) and EC (14.7-37.4%) mainly due to the incomplete combustion of fuels. In addition, the chemical components proportions of PM emitted from the same industry source also vary with the application of different complex production processes (such as the iron & steel industry) and/or different fuel types (such as the power industry).

The concentrations of toxic trace elements in PMs emitted from major anthropogenic sources are shown in Fig. 4. The targeted toxic elements include Be, Sc, Ti, V, Cr, Mn, Fe, Al, Co, Ni, Cu, Zn, Ga, Ge, As, Se, Rb, Sr, Mo, Cd, Sn, Sb, Cs, Ba, Tl, and Pb. Industrial sources-emitted PM has much higher concentrations of toxic elements than those of residential (15.6 times) and transportation (10.8 times for tailpipe exhaust and 3.8 times for non-exhaust) sources-emitted PM (Fig. 4a). Furthermore, the concentrations of toxic elements in per unit mass of PMs emitted from the iron & steel industry (253.0 ± 98.0 mg/g) and non-ferrous metal smelting industry (328.1 ± 222.3 mg/g) are substantially higher than those emitted from other industrial sources (27.4 ± 23.1 mg/g), due to their high contents in raw materials. The average concentrations of these concerned toxic elements in PMs emitted from the iron & steel industry are approximately 10.9, 4.6, 8.8, and 20.4-55.1 times of that in PMs emitted from the power industry, industrial boilers, cement industry, and other sources, respectively. Figure 4b illustrates the average concentrations of individual toxic elements in per unit mass of source-specific PMs. Fe predominates the mass concentrations of PM-bound elements among most emission sectors, with average mass concentration ranging from 0.4 to 270.1 mg/g per unit mass of PM, and mass fraction ranging from 21.3 to 96.7% of all targeted toxic elements. The concentrations of other elements vary among different sectors. For example, the highest mass concentrations of PM-bound Cu, Zn, Ni, As, Cd, and Pb are observed in the non-ferrous metal smelting industry. Additionally, the residential burning of anthracite coal exhibits the highest mass concentration of Se, while non-exhaust emissions from vehicles and the non-ferrous metal smelting industry show a relatively higher concentration of Sb.

The total concentrations of 16 PAHs contained in PMs from different emission sources are shown in Fig. 5a. The concentrations of PM-bound PAHs from the residential (coal and biomass burning: 5967.7 ± 5520.2 μg/g)

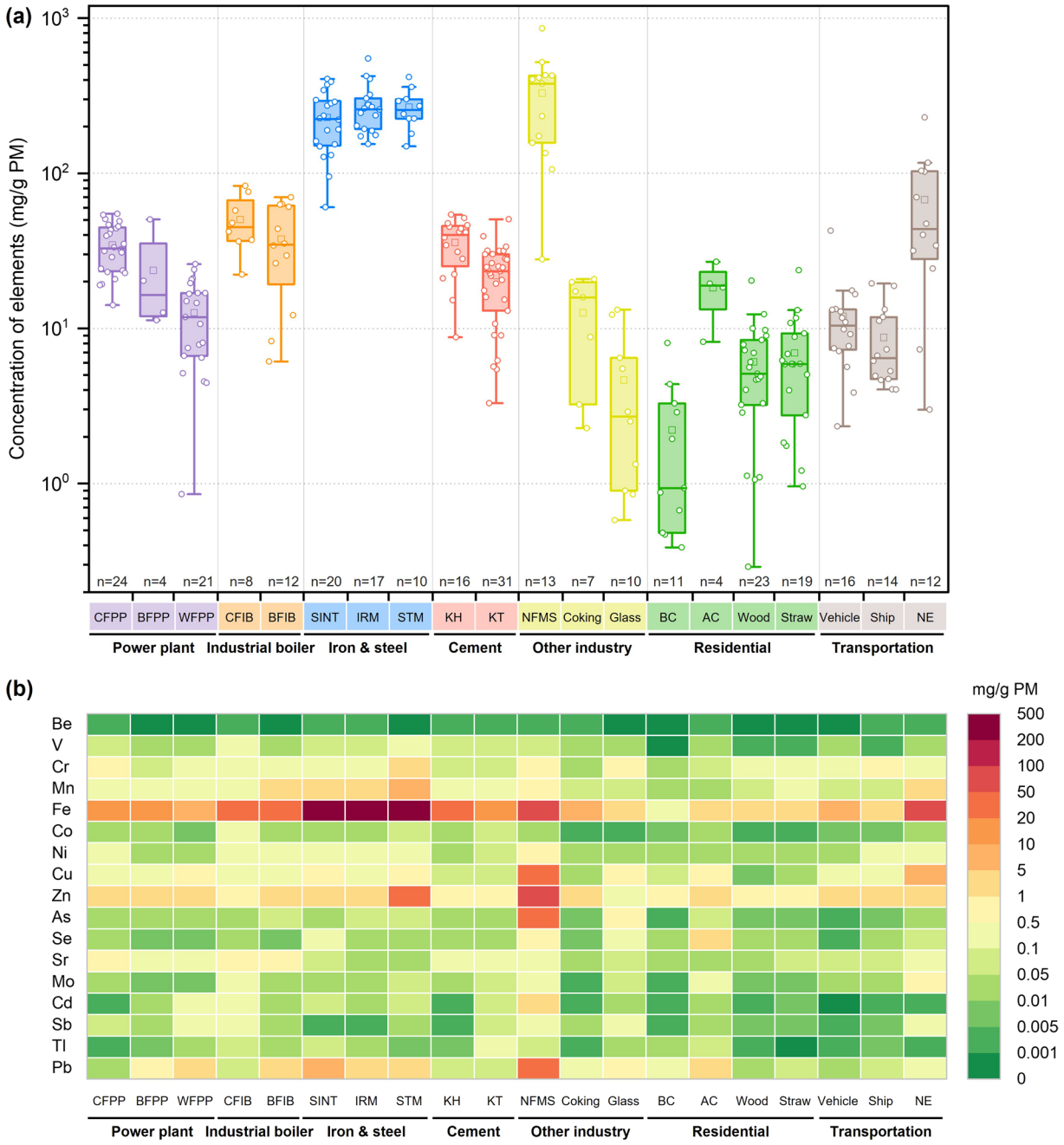

Fig. 4 Concentrations of toxic elements in PM emitted from typical anthropogenic emission sources. (**a**) The total mass-normalized concentrations of toxic elements (i.e., Be, Sc, Ti, V, Cr, Mn, Fe, Al, Co, Ni, Cu, Zn, Ga, Ge, As, Se, Rb, Sr, Mo, Cd, Sn, Sb, Cs, Ba, Tl, and Pb) in PM. (**b**) The concentrations of individual toxic elements per unit mass of PM originating from different emission sources. CFPP: coal-fired power plants; BFPP: biomass-fired power plants; WFPP: solid waste-fired power plants; CFIB: coal-fired industrial boilers; BFIB: biomass-fired industrial boilers; SINT: sintering; IRM: ironmaking; STM: steelmaking; KH: kiln head; KT: kiln tail; NFMS: non-ferrous metal smelting; BC: bituminous coal; AC: anthracite coal. In addition, "Vehicle" and "Ship" indicate exhaust emission, while "NE" means non-exhaust emission.

and transportation (tailpipe exhaust: $219.1 \pm 310.8\,\mu g/g$) emissions are approximately 1-2 orders of magnitude higher than those from industrial sources (except iron & steel industry). Among these industrial sources, the iron & steel industry contains the highest average content of PM-bound PAHs ($622.5 \pm 747.5\,\mu g/g$), which is about 22.7 times larger than the power industry ($27.7 \pm 39.2\,\mu g/g$). In addition, the average concentration of 16 priority PAHs per unit mass of PMs is exhibited in Fig. 5b. The 16 PAHs have relatively higher concentrations in PMs emitted from residential coal and biomass burning, tailpipe exhaust of ship, and iron & steel industry. The dominant species of PAHs in PM also exhibits discrepancies among emission sectors. For example, the

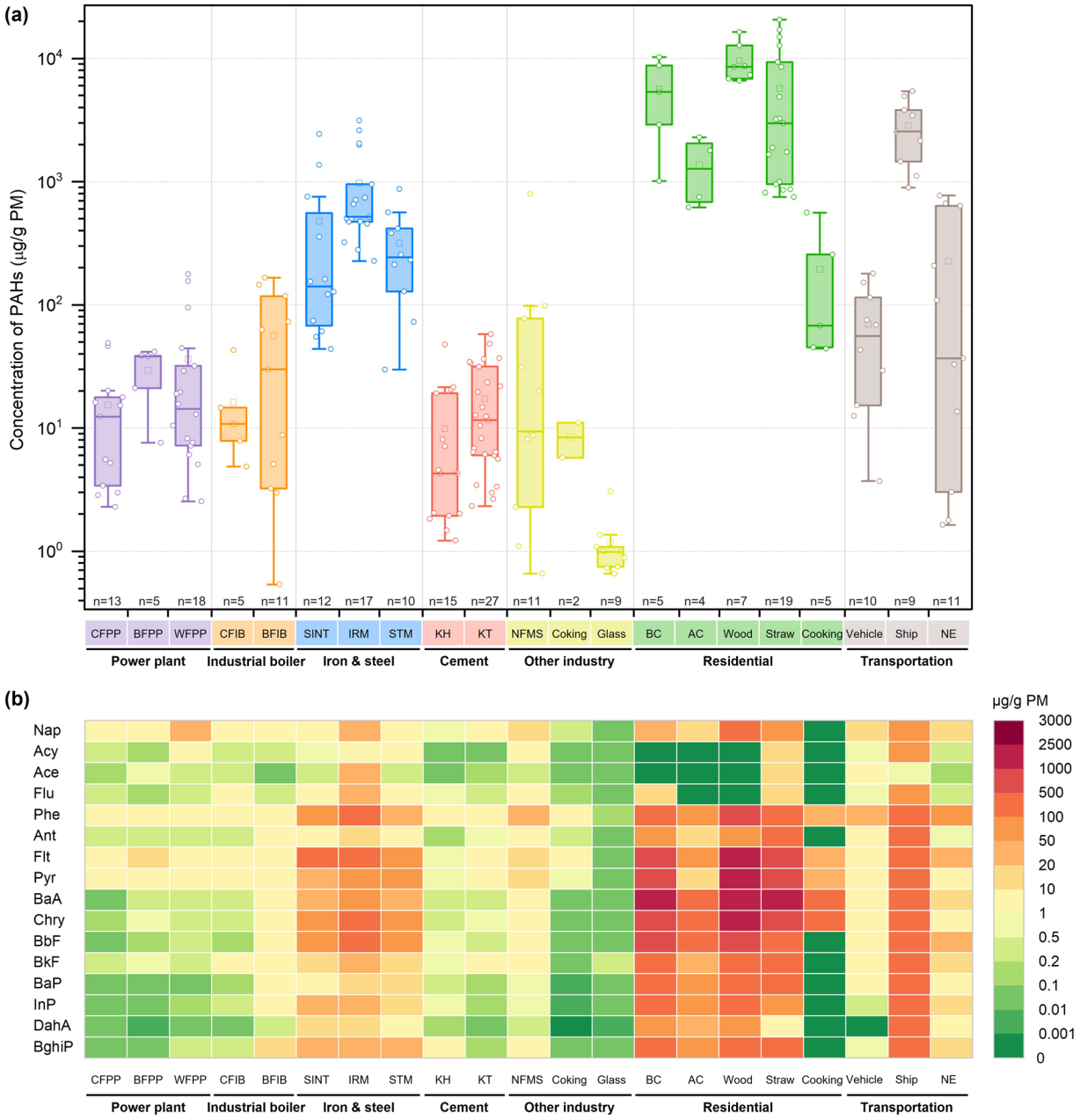

Fig. 5 Concentrations of PAHs in PM emitted from typical anthropogenic emission sources. (**a**) The total mass-normalized concentrations of 16 PAHs in PM. (**b**) The concentrations of individual PAH per unit mass of PM originating from different emission sources. CFPP: coal-fired power plants; BFPP: biomass-fired power plants; WFPP: solid waste-fired power plants; CFIB: coal-fired industrial boilers; BFIB: biomass-fired industrial boilers; SINT: sintering; IRM: ironmaking; STM: steelmaking; KH: kiln head; KT: kiln tail; NFMS: non-ferrous metal smelting; BC: bituminous coal; AC: anthracite coal. In addition, "Vehicle" and "Ship" indicate exhaust emission, while "NE" means non-exhaust emission.

dominant species of PM-bound PAHs emitted from iron & steel industry are Flt, BbF, and Phe, while the dominant species from residential biomass burning are BaA, Chry, and Flt.

In addition, a brief summary of major PM-bound chemical species based on typical emission source classifications from this dataset is shown in Supplementary Tables S1–S7, which provide averages, standard deviations, interquartile ranges (IQR), medians, and range levels for uncertainty assessment reference.

Comparisons of emission data with other studies. In this section of the data descriptor, source-specific elements and PAHs of PM samples in our dataset were chosen to make comparisons with those reported in previous studies. Four industrial sectors, including the power industry (with fuel types of coal[23,25,58–60], biomass[61], and solid waste[25,58]), industrial boilers[23,62], the iron & steel industry[63,64], and cement industry[27], and residential sectors (including coal and biomass burning[19,65–67]), and transportation sector (including tailpipe exhaust of vehicle

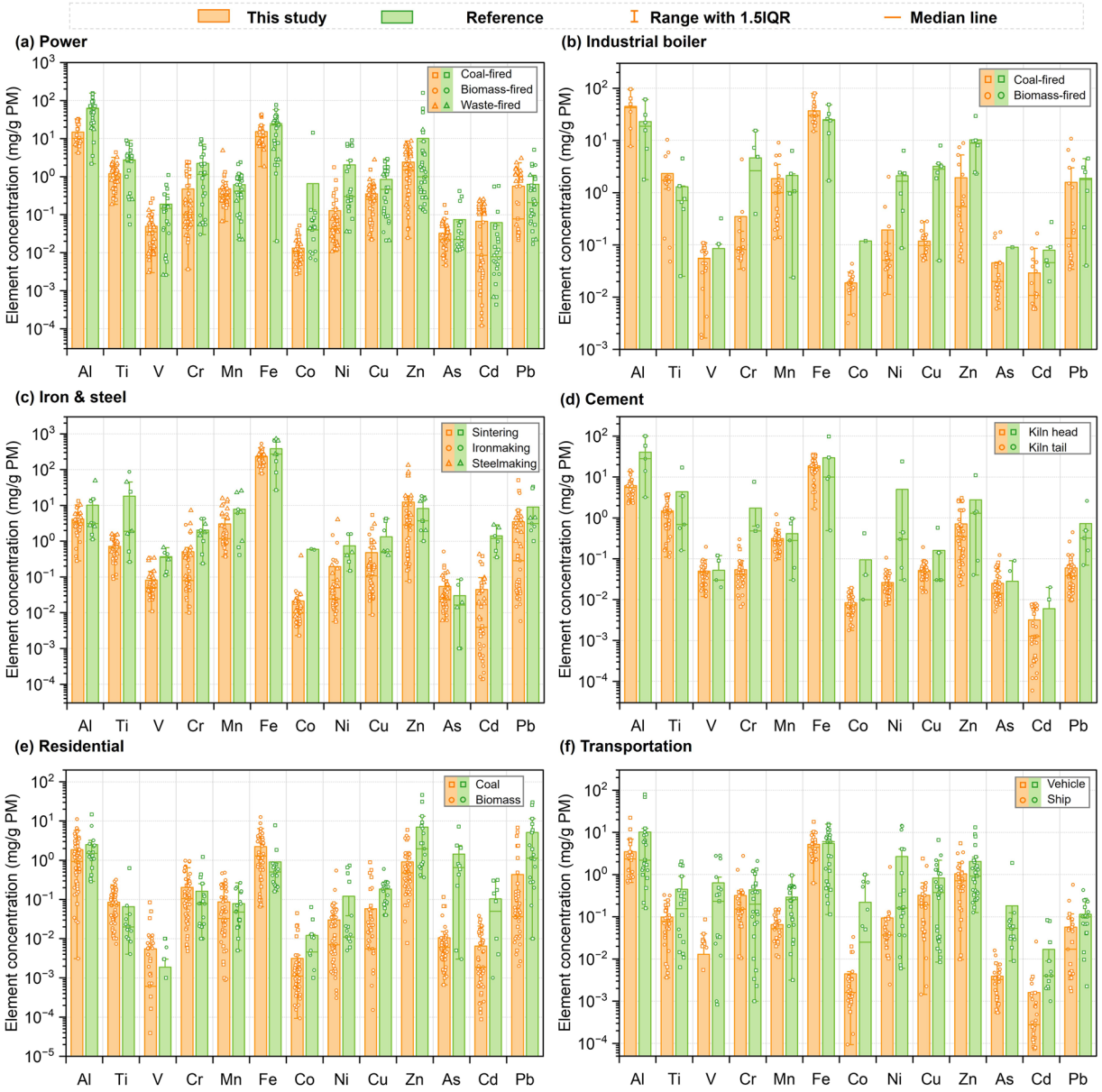

Fig. 6 Comparison of source-specific PM-bound elements with previous studies. The concentrations of elements in PM emitted from (**a**) power industry involving coal-fired power plants[23,25,58–60], biomass-fired power plants[61] and waste-fired power plants[25,58], (**b**) industrial boilers[23,62], (**c**) iron & steel industry[63,64], (**d**) cement industry including kiln head and kiln tail processes[27], (**e**) residential sector including coal and biomass burning[19,65–67], and (**f**) transportation sector involving tailpipe exhaust of vehicle and ship[23,25,26,60,68–71].

and ship[23,25,26,60,68–71]), were selected to conduct data comparison with previous studies. Due to the limitation on the number of element species from other available published data, only a part of the elements was listed in this section. In addition, the total concentrations of PAHs and their BaP_{eq} values in industrial sectors (including power industry[22,72–74], iron & steel industry[22,72], and cement industry[72]), residential sectors (including coal[75–78], biomass burning[21,67,78–80], and cooking emission[81]), and transportation sectors (including exhaust of vehicles and ships[68,82–84], and non-exhaust emission from vehicles[85,86]) were selected to make comparison with other studies, which could comprehensively reflect the overall level of source-specific PAHs and their carcinogenic potency.

As shown in Figs. 6 and 7, the concentrations of PM-bound elements, PAHs, and their corresponding Bap_{eq} value in this study show similar trends with other studies among emission sectors. An additional comparison of WSIs with other studies was summarized in Supplementary Table S8, indicating similar ranges for the main WSIs.

The data on individual species and emission sources in this study generally align with those reported in previous studies, largely within one order of magnitude. The discrepancy of certain chemical species with previous studies possibly resulted from the uncertainty of various field conditions, sampling, and detecting methods. The chemical profiles of source-specific PM can provide valuable data in source apportionment, emission

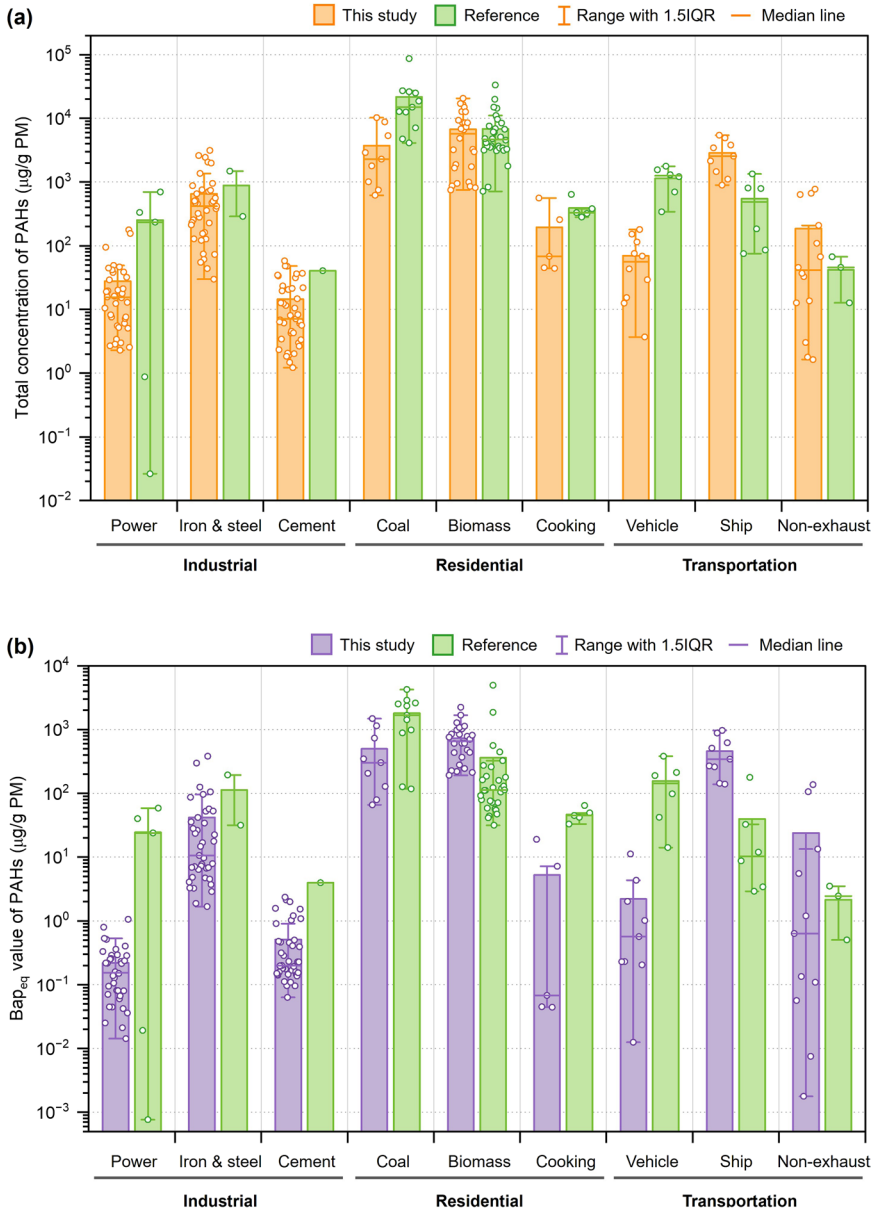

Fig. 7 Comparison of source-specific PM-bound PAHs with previous studies. The total concentration of PAHs (**a**) and corresponding BaP_{eq} values (**b**) of the industrial sector (including power industry[22,72–74], iron & steel industry[22,72], and cement industry[72]), residential sector (involving coal burning[75–78], biomass burning[21,67,78–80], and cooking emission[81]), and transportation sector (including tailpipe exhaust of vehicles and ships[68,82–84], and non-exhaust emission from vehicles[85,86]).

inventory studies, and health risk estimation and serve as fundamental input data for atmospheric chemistry transport models, enabling a deeper understanding of the potential effects resulting from ambient PM pollution. Considering the local features of source profiles, establishing detailed local source profiles and emission inventories across China is necessary and important. However, it requires considerable effort to achieve this goal. Additionally, the integration of results from different researchers necessitates the adoption of standard methods, such as field sampling and measurements of chemical components to minimize the uncertainty resulting from variations in study approaches.

Usage Notes

Industrial PM samples in this study refer to the filterable PM, which refers to particles that are directly emitted as a solid or liquid at stack condition. Consequently, relying solely on this dataset to quantify total pollutants emitted from industrial entire flue gases could underestimate certain chemicals that readily disperse into the gas phase.

Although the sampling covers a wide geographic and source category in China, it doesn't cover all potential variation in emission profiles across different regions and over time. More extensive investigations in the future

or complementarity with other research data are needed to address this issue. When determining the emission factor for one specific source, it is important to consider the applicability of the available data, such as the similarity of emission units evaluated within a specific area or data quality. In some cases, the emission factor may be chosen as representative source-specific range level, or even simply as the average and median of available data of acceptable quality for the same source category. Uncertainty analysis, evaluated through the propagation of error and the Monte Carlo method[18,37,87], should be conducted especially when integrating the data further with other emission inventories or models.

Varied methodologies for collecting and processing emission data could result in inconsistencies in how emissions are quantified and categorized. The quality of data also influences the accuracy of integrated analyses, given the uncertainties induced. For example, the emission factor of the PM mass-based dataset can be integrated with other inventories with PM emission data. However, the used subcategory of emission source in this study cannot exactly match with all inventories. Thus, it is crucial to establish clear and standardized guidelines or standards for data collection, reporting and integration. To address the data gaps or anomalies, potential statistical techniques will be required to be employed. Moreover, sensitivity analyses and scenario assessments can quantify how integrating data affects emission estimates and model outcomes. Finally, continuous efforts should be made to establish common data repositories or platforms, enabling more precise integrated analyses with high resolution.

Code availability

No custom code was used in the generation of the dataset. Microsoft Excel and Origin were employed to process data and draw the figures in this descriptor.

Received: 13 February 2024; Accepted: 31 October 2024;
Published online: 08 November 2024

References

1. Lelieveld, J., Evans, J. S., Fnais, M., Giannadaki, D. & Pozzer, A. The contribution of outdoor air pollution sources to premature mortality on a global scale. *Nature* **525**, 367–371, https://doi.org/10.1038/nature15371 (2015).
2. Al-Kindi, S. G., Brook, R. D., Biswal, S. & Rajagopalan, S. Environmental determinants of cardiovascular disease: lessons learned from air pollution. *Nat. Rev. Cardiol.* **17**, 656–672, https://doi.org/10.1038/s41569-020-0371-2 (2020).
3. Hill, W. *et al*. Lung adenocarcinoma promotion by air pollutants. *Nature* **616**, 159–167, https://doi.org/10.1038/s41586-023-05874-3 (2023).
4. Burnett, R. T. *et al*. An integrated risk function for estimating the global burden of disease attributable to ambient fine particulate matter exposure. *Environ. Health Perspect.* **122**, 397–403, https://doi.org/10.1289/ehp.1307049 (2014).
5. Seinfeld, J. H. & Pandis, S. N. *Atmospheric Chemistry and Physics: From Air Pollution to Climate Change*. 3rd edn, (New York: Wiley Press, 2016).
6. Lepeule, J., Laden, F., Dockery, D. & Schwartz, J. Chronic exposure to fine particles and mortality: An extended follow-up of the Harvard Six Cities study from 1974 to 2009. *Environ. Health Perspect.* **120**, 965–970, https://doi.org/10.1289/ehp.1104660 (2012).
7. Pope, C. A. *et al*. Relationships between fine particulate air pollution, cardiometabolic disorders, and cardiovascular mortality. *Circ. Res.* **116**, 108–115, https://doi.org/10.1161/CIRCRESAHA.116.305060 (2015).
8. Cohen, A. J. *et al*. Estimates and 25-year trends of the global burden of disease attributable to ambient air pollution: an analysis of data from the Global Burden of Diseases Study 2015. *The Lancet* **389**, 1907–1918, https://doi.org/10.1016/S0140-6736(17)30505-6 (2017).
9. Li, X.-D., Jin, L. & Kan, H. Air pollution: a global problem needs local fixes. *Nature* **570**, 437–439, https://doi.org/10.1038/d41586-019-01960-7 (2019).
10. Kelly, F. J. & Fussell, J. C. Size, source and chemical composition as determinants of toxicity attributable to ambient particulate matter. *Atmos. Environ.* **60**, 504–526, https://doi.org/10.1016/j.atmosenv.2012.06.039 (2012).
11. Wu, D. *et al*. Toxic potency-adjusted control of air pollution for solid fuel combustion. *Nat. Energy* **7**, 194–202, https://doi.org/10.1038/s41560-021-00951-1 (2022).
12. Jin, L. *et al*. Contributions of city-specific fine particulate matter ($PM_{2.5}$) to differential *in vitro* oxidative stress and toxicity implications between Beijing and Guangzhou of China. *Environ. Sci. Technol.* **53**, 2881–2891, https://doi.org/10.1021/acs.est.9b00449 (2019).
13. Wu, D. *et al*. More than concentration reduction: Contributions of oxidation technologies to alleviating aerosol toxicity from diesel engines. *Environ. Sci. Technol. Lett.* **9**, 280–285, https://doi.org/10.1021/acs.estlett.2c00069 (2022).
14. Tang, L. *et al*. Substantial emission reductions from Chinese power plants after the introduction of ultra-low emissions standards. *Nat. Energy* **4**, 929–938, https://doi.org/10.1038/s41560-019-0468-1 (2019).
15. Ding, X. *et al*. Unexpectedly increased particle emissions from the steel industry determined by wet/semidry/dry flue gas desulfurization technologies. *Environ. Sci. Technol.* **53**, 10361–10370, https://doi.org/10.1021/acs.est.9b03081 (2019).
16. Wu, D. *et al*. Primary particulate matter emitted from heavy fuel and diesel oil combustion in a typical container ship: characteristics and toxicity. *Environ. Sci. Technol.* **52**, 12943–12951, https://doi.org/10.1021/acs.est.8b04471 (2018).
17. Wu, D. *et al*. Achieving health-oriented air pollution control requires integrating unequal toxicities of industrial particles. *Nat. Commun.* **14**, 6491, https://doi.org/10.1038/s41467-023-42089-6 (2023).
18. Li, M. *et al*. Anthropogenic emission inventories in China: A review. *Natl. Sci. Rev.* **4**, 834–866, https://doi.org/10.1093/nsr/nwx150 (2017).
19. Ge, S. *et al*. Emissions of air pollutants from household stoves: honeycomb coal versus coal cake. *Environ. Sci. Technol.* **38**, 4612–4618, https://doi.org/10.1021/es049942k (2004).
20. Zhao, Y., Wang, S., Nielsen, C. P., Li, X. & Hao, J. Establishment of a database of emission factors for atmospheric pollutants from Chinese coal-fired power plants. *Atmos. Environ.* **44**, 1515–1523, https://doi.org/10.1016/j.atmosenv.2010.01.017 (2010).
21. Shen, G. *et al*. Emissions of PAHs from indoor crop residue burning in a typical rural stove: Emission factors, size distributions, and gas-particle partitioning. *Environ. Sci. Technol.* **45**, 1206–1212, https://doi.org/10.1021/es102151w (2011).
22. Kong, S. *et al*. Characterization of PAHs within PM_{10} fraction for ashes from coke production, iron smelt, heating station and power plant stacks in Liaoning Province, China. *Atmos. Environ.* **45**, 3777–3785, https://doi.org/10.1016/j.atmosenv.2011.04.029 (2011).
23. Bi, X. *et al*. Characteristics of the main primary source profiles of particulate matter across China from 1987 to 2017. *Atmos. Chem. Phys.* **19**, 3223–3243, https://doi.org/10.5194/acp-19-3223-2019 (2019).
24. Liu, Y., Xing, J., Wang, S., Fu, X. & Zheng, H. Source-specific speciation profiles of $PM_{2.5}$ for heavy metals and their anthropogenic emissions in China. *Environ. Pollut* **239**, 544–553, https://doi.org/10.1016/j.envpol.2018.04.047 (2018).

25. Chen, P. *et al.* Characterization of major natural and anthropogenic source profiles for size-fractionated PM in Yangtze River Delta. *Sci. Total Environ.* **598**, 135–145, https://doi.org/10.1016/j.scitotenv.2017.04.106 (2017).
26. Zhang, Y., Yao, Z., Shen, X., Liu, H. & He, K. Chemical characterization of $PM_{2.5}$ emitted from on-road heavy-duty diesel trucks in China. *Atmos. Environ.* **122**, 885–891, https://doi.org/10.1016/j.atmosenv.2015.07.014 (2015).
27. Guo, Z. *et al.* Field measurements on emission characteristics, chemical profiles, and emission factors of size-segregated PM from cement plants in China. *Sci. Total Environ.* **818**, 151822, https://doi.org/10.1016/j.scitotenv.2021.151822 (2022).
28. Li, Q. *et al.* Gaseous ammonia emissions from coal and biomass combustion in household stoves with different combustion efficiencies. *Environ. Sci. Technol. Lett.* **3**, 98–103, https://doi.org/10.1021/acs.estlett.6b00013 (2016).
29. Liu, Y. *et al.* Particulate matter, gaseous and particulate polycyclic aromatic hydrocarbons (PAHs) in an urban traffic tunnel of China: Emission from on-road vehicles and gas-particle partitioning. *Chemosphere* **134**, 52–59, https://doi.org/10.1016/j.chemosphere.2015.03.065 (2015).
30. Zheng, B. *et al.* Trends in China's anthropogenic emissions since 2010 as the consequence of clean air actions. *Atmos. Chem. Phys.* **18**, 14095–14111, https://doi.org/10.5194/acp-18-14095-2018 (2018).
31. An, J. *et al.* Emission inventory of air pollutants and chemical speciation for specific anthropogenic sources based on local measurements in the Yangtze River Delta region, China. *Atmos. Chem. Phys.* **21**, 2003–2025, https://doi.org/10.5194/acp-21-2003-2021 (2021).
32. Fu, X. *et al.* Emission inventory of primary pollutants and chemical speciation in 2010 for the Yangtze River Delta region, China. *Atmos. Environ.* **70**, 39–50, https://doi.org/10.1016/j.atmosenv.2012.12.034 (2013).
33. Zhu, C. *et al.* A high-resolution emission inventory of anthropogenic trace elements in Beijing-Tianjin-Hebei (BTH) region of China. *Atmos. Environ.* **191**, 452–462, https://doi.org/10.1016/j.atmosenv.2018.08.035 (2018).
34. Hua, S. *et al.* Atmospheric emission inventory of hazardous air pollutants from China's cement plants: Temporal trends, spatial variation characteristics and scenario projections. *Atmos. Environ.* **128**, 1–9, https://doi.org/10.1016/j.atmosenv.2015.12.056 (2016).
35. Tian, H. Z. *et al.* Quantitative assessment of atmospheric emissions of toxic heavy metals from anthropogenic sources in China: historical trend, spatial distribution, uncertainties, and control policies. *Atmos. Chem. Phys.* **15**, 10127–10147, https://doi.org/10.5194/acp-15-10127-2015 (2015).
36. Liu, F. *et al.* High-resolution inventory of technologies, activities, and emissions of coal-fired power plants in China from 1990 to 2010. *Atmos. Chem. Phys.* **15**, 13299–13317, https://doi.org/10.5194/acp-15-13299-2015 (2015).
37. Zhao, Y., Nielsen, C. P., Lei, Y., McElroy, M. B. & Hao, J. Quantifying the uncertainties of a bottom-up emission inventory of anthropogenic atmospheric pollutants in China. *Atmos. Chem. Phys.* **11**, 2295–2308, https://doi.org/10.5194/acp-11-2295-2011 (2011).
38. Shen, H. *et al.* A critical review of pollutant emission factors from fuel combustion in home stoves. *Environ. Int.* **157**, 106841, https://doi.org/10.1016/j.envint.2021.106841 (2021).
39. Tang, L. *et al.* Chinese industrial air pollution emissions based on the continuous emission monitoring systems network. *Sci. Data* **10**, 153, https://doi.org/10.1038/s41597-023-02054-w (2023).
40. Yun, X. *et al.* Residential solid fuel emissions contribute significantly to air pollution and associated health impacts in China. *Sci. Adv.* **6**, eaba7621, https://doi.org/10.1126/sciadv.aba7621 (2020).
41. Wu, Y. *et al.* On-road vehicle emissions and their control in China: A review and outlook. *Sci. Total Environ.* **574**, 332–349, https://doi.org/10.1016/j.scitotenv.2016.09.040 (2017).
42. Shen, G. *et al.* Emission characteristics for polycyclic aromatic hydrocarbons from solid fuels burned in domestic stoves in rural China. *Environ. Sci. Technol.* **47**, 14485–14494, https://doi.org/10.1021/es403110b (2013).
43. Zheng, L. *et al.* Chemical Profiles of Primary Particulate Matter Emitted from Typical Anthropogenic Sources in Selected Regions of China. *figshare* https://doi.org/10.6084/m9.figshare.27139740 (2024).
44. Ding, X. *et al.* Gaseous and particulate chlorine emissions from typical iron and steel industry in China. *J. Geophys. Res.: Atmos.* **125**, e2020JD032729, https://doi.org/10.1029/2020JD032729 (2020).
45. Zhang, J. *et al.* Emission characteristics of heavy metals from a typical copper smelting plant. *J. Hazard. Mater.* **424**, 127311, https://doi.org/10.1016/j.jhazmat.2021.127311 (2022).
46. Liang, Y. *et al.* Forward ultra-low emission for power plants via wet electrostatic precipitators and newly developed demisters: Filterable and condensable particulate matters. *Atmos. Environ.* **225**, 117372, https://doi.org/10.1016/j.atmosenv.2020.117372 (2020).
47. Wu, D. *et al.* Extreme exposure levels of PCDD/Fs inhaled from biomass burning activity for cooking in typical rural households. *Environ. Sci. Technol.* **55**, 7299–7306, https://doi.org/10.1021/acs.est.1c00469 (2021).
48. Huo, Y. *et al.* Addressing unresolved complex mixture of I/SVOCs emitted From incomplete combustion of solid fuels by nontarget analysis. *J. Geophys. Res.: Atmos.* **126**, e2021JD035835, https://doi.org/10.1029/2021JD035835 (2021).
49. Guo, Z. *et al.* Higher toxicity of gaseous organics relative to particulate matters emitted from typical cooking processes. *Environ. Sci. Technol.* **57**, 17022–17031, https://doi.org/10.1021/acs.est.3c05425 (2023).
50. Chow, J. C. *et al.* The IMPROVE_A temperature protocol for thermal/optical carbon analysis: maintaining consistency with a long-term database. *J. Air Waste Manage. Assoc.* **57**, 1014–1023, https://doi.org/10.3155/1047-3289.57.9.1014 (2007).
51. Wu, D. *et al.* Commodity plastic burning as a source of inhaled toxic aerosols. *J. Hazard. Mater.* **416**, 125820, https://doi.org/10.1016/j.jhazmat.2021.125820 (2021).
52. Delistraty Ph.D, D. A. B. T. D. Toxic equivalency factor approach for risk assessment of polycyclic aromatic hydrocarbons. *Toxicol. Environ. Chem.* **64**, 81-108, https://doi.org/10.1080/02772249709358542 (1997).
53. Nisbet, I. C. T. & LaGoy, P. K. Toxic equivalency factors (TEFs) for polycyclic aromatic hydrocarbons (PAHs). *Regul. Toxicol. Pharmacol.* **16**, 290–300, https://doi.org/10.1016/0273-2300(92)90009-X (1992).
54. Wu, D. *et al.* Source analysis and health risk assessment of polycyclic aromatic hydrocarbon (PAHs) in total suspended particulate matter (TSP) from Bengbu, China. *Sci. Rep.* **14**, 5080, https://doi.org/10.1038/s41598-024-55695-1 (2024).
55. Yan, D. *et al.* Characteristics, sources and health risk assessment of airborne particulate PAHs in Chinese cities: A review. *Environ. Pollut* **248**, 804–814, https://doi.org/10.1016/j.envpol.2019.02.068 (2019).
56. Chen, Y.-W., Liu, K.-T., Thi Phuong Thao, H., Jian, M.-Y. & Cheng, Y.-H. Insight into the diurnal variations and potential sources of ambient PM2.5-bound polycyclic aromatic hydrocarbons during spring in Northern Taiwan. *J. Hazard. Mater.* **476**, 134977, https://doi.org/10.1016/j.jhazmat.2024.134977 (2024).
57. Li, S. *et al.* Emission trends of air pollutants and CO_2 in China from 2005 to 2021. *Earth Syst. Sci. Data* **15**, 2279–2294, https://doi.org/10.5194/essd-15-2279-2023 (2023).
58. Zeng, X. *et al.* Source profiles and emission factors of organic and inorganic species in fine particles emitted from the ultra-low emission power plant and typical industries. *Sci. Total Environ.* **789**, 147966, https://doi.org/10.1016/j.scitotenv.2021.147966 (2021).
59. Chen, X. *et al.* Emission characteristics of fine particulate matter from ultra-low emission power plants. *Environ. Pollut* **255**, 113157, https://doi.org/10.1016/j.envpol.2019.113157 (2019).
60. Zhang, N. *et al.* Development of source profiles and their application in source apportionment of $PM_{2.5}$ in Xiamen, China. *Front. Environ. Sci. Eng.* **10**, 17, https://doi.org/10.1007/s11783-016-0879-1 (2016).
61. Wang, X. *et al.* Characteristics of ash and slag from four biomass-fired power plants: Ash/slag ratio, unburned carbon, leaching of major and trace elements. *Energy Convers. Manage.* **214**, 112897, https://doi.org/10.1016/j.enconman.2020.112897 (2020).

62. Pei, B. *et al*. Emissions and source profiles of $PM_{2.5}$ for coal-fired boilers in the Shanghai megacity, China. *Atmos. Pollut. Res.* **7**, 577–584, https://doi.org/10.1016/j.apr.2016.01.005 (2016).
63. Guo, Y., Gao, X., Zhu, T., Luo, L. & Zheng, Y. Chemical profiles of PM emitted from the iron and steel industry in northern China. *Atmos. Environ.* **150**, 187–197, https://doi.org/10.1016/j.atmosenv.2016.11.055 (2017).
64. Jia, J. *et al*. Emission characteristics and chemical components of size-segregated particulate matter in iron and steel industry. *Atmos. Environ.* **182**, 115–127, https://doi.org/10.1016/j.atmosenv.2018.03.051 (2018).
65. Dai, Q. *et al*. Residential coal combustion as a source of primary sulfate in Xi'an, China. *Atmos. Environ.* **196**, 66–76, https://doi.org/10.1016/j.atmosenv.2018.10.002 (2019).
66. Zhang, H. *et al*. Chemical and size characterization of particles emitted from the burning of coal and wood in rural households in Guizhou, China. *Atmos. Environ.* **51**, 94–99, https://doi.org/10.1016/j.atmosenv.2012.01.042 (2012).
67. Sun, J. *et al*. Effects of biomass briquetting and carbonization on $PM_{2.5}$ emission from residential burning in Guanzhong Plain, China. *Fuel* **244**, 379–387, https://doi.org/10.1016/j.fuel.2019.02.031 (2019).
68. Cui, M. *et al*. Measurement of PM and its chemical composition in real-world emissions from non-road and on-road diesel vehicles. *Atmos. Chem. Phys.* **17**, 6779–6795, https://doi.org/10.5194/acp-17-6779-2017 (2017).
69. Hao, Y. *et al*. Chemical characterisation of $PM_{2.5}$ emitted from motor vehicles powered by diesel, gasoline, natural gas and methanol fuel. *Sci. Total Environ.* **674**, 128–139, https://doi.org/10.1016/j.scitotenv.2019.03.410 (2019).
70. Zhang, J. *et al*. Vehicular non-exhaust particulate emissions in Chinese megacities: Source profiles, real-world emission factors, and inventories. *Environ. Pollut* **266**, 115268, https://doi.org/10.1016/j.envpol.2020.115268 (2020).
71. Wen, J. *et al*. PM2.5 source profiles and relative heavy metal risk of ship emissions: Source samples from diverse ships, engines, and navigation processes. *Atmos. Environ.* **191**, 55–63, https://doi.org/10.1016/j.atmosenv.2018.07.038 (2018).
72. Kong, S., Ji, Y., Li, Z., Lu, B. & Bai, Z. Emission and profile characteristic of polycyclic aromatic hydrocarbons in $PM_{2.5}$ and PM_{10} from stationary sources based on dilution sampling. *Atmos. Environ.* **77**, 155–165, https://doi.org/10.1016/j.atmosenv.2013.04.073 (2013).
73. Wang, R., Liu, G. & Zhang, J. Variations of emission characterization of PAHs emitted from different utility boilers of coal-fired power plants and risk assessment related to atmospheric PAHs. *Sci. Total Environ.* **538**, 180–190, https://doi.org/10.1016/j.scitotenv.2015.08.043 (2015).
74. Li, Z. *et al*. Characterization of PAHs and PCBs in Fly Ashes of Eighteen Coal-Fired Power Plants. *Aerosol Air Qual. Res.* **16**, 3175–3186, https://doi.org/10.4209/aaqr.2016.10.0430 (2016).
75. Li, Q. *et al*. Improving the energy efficiency of stoves to reduce pollutant emissions from household solid fuel combustion in China. *Environ. Sci. Technol. Lett.* **3**, 369–374, https://doi.org/10.1021/acs.estlett.6b00324 (2016).
76. Zhang, Y. *et al*. Characteristics of particulate carbon emissions from real-world Chinese coal combustion. *Environ. Sci. Technol.* **42**, 5068–5073, https://doi.org/10.1021/es7022576 (2008).
77. Shen, G. *et al*. Emission factors and particulate matter size distribution of polycyclic aromatic hydrocarbons from residential coal combustions in rural Northern China. *Atmos. Environ.* **44**, 5237–5243, https://doi.org/10.1016/j.atmosenv.2010.08.042 (2010).
78. Shen, G. *et al*. Emission factors of particulate matter and elemental carbon for crop residues and coals burned in typical household stoves in China. *Environ. Sci. Technol.* **44**, 7157–7162, https://doi.org/10.1021/es101313y (2010).
79. Shen, G. *et al*. Emission factors, size distributions, and emission inventories of carbonaceous particulate matter from residential wood combustion in rural China. *Environ. Sci. Technol.* **46**, 4207–4214, https://doi.org/10.1021/es203957u (2012).
80. Shen, G. *et al*. Emissions of parent, nitro, and oxygenated polycyclic aromatic hydrocarbons from residential wood combustion in rural China. *Environ. Sci. Technol.* **46**, 8123–8130, https://doi.org/10.1021/es301146v (2012).
81. Li, Y.-C. *et al*. Characteristics of polycyclic aromatic hydrocarbons in $PM_{2.5}$ emitted from different cooking activities in China. *Environ. Sci. Pollut. Res.* **25**, 4750–4760, https://doi.org/10.1007/s11356-017-0603-0 (2018).
82. Zheng, X. *et al*. Measurement of particulate polycyclic aromatic hydrocarbon emissions from gasoline light-duty passenger vehicles. *J. Cleaner Prod.* **185**, 797–804, https://doi.org/10.1016/j.jclepro.2018.03.078 (2018).
83. Zhao, J. *et al*. Characterization of $PM_{2.5}$-bound polycyclic aromatic hydrocarbons and their derivatives (nitro-and oxy-PAHs) emissions from two ship engines under different operating conditions. *Chemosphere* **225**, 43–52, https://doi.org/10.1016/j.chemosphere.2019.03.022 (2019).
84. Yang, L. *et al*. Real world emission characteristics of Chinese fleet and the current situation of underestimated ship emissions. *J. Cleaner Prod.* **418**, 138107, https://doi.org/10.1016/j.jclepro.2023.138107 (2023).
85. Alves, C. A. *et al*. Physical and chemical properties of non-exhaust particles generated from wear between pavements and tyres. *Atmos. Environ.* **224**, 117252, https://doi.org/10.1016/j.atmosenv.2019.117252 (2020).
86. Kreider, M. L., Panko, J. M., McAtee, B. L., Sweet, L. I. & Finley, B. L. Physical and chemical characterization of tire-related particles: Comparison of particles generated using different methodologies. *Sci. Total Environ.* **408**, 652–659, https://doi.org/10.1016/j.scitotenv.2009.10.016 (2010).
87. Kurokawa, J. *et al*. Emissions of air pollutants and greenhouse gases over Asian regions during 2000–2008: Regional Emission inventory in ASia (REAS) version 2. *Atmos. Chem. Phys.* **13**, 11019–11058, https://doi.org/10.5194/acp-13-11019-2013 (2013).

Acknowledgements

We thank Yuzhe Liu, Yuanzheng Chen, Jiaying Xu, Dr. Xiang Ding, Dr. Yaoqiang Huo, Dr. Anlin Liu, and Shuya Li, from Fudan University for supporting the field sampling. This work was supported by the National Natural Science Foundation of China (U22A20405 and T2122006), the Ministry of Science and Technology of China (2022YFC3700501), and China Postdoctoral Science Foundation (BX20220088 and 2022M710741).

Author contributions

Q.L. and D.W. conceived and designed the experiments. L.Z., D.W., X.C., A.C. and J.Y. performed the experiments. L.Z., D.W., X.C. and Y.L. analyzed the data and prepared graphs; L.Z., D.W., X.C. and Y.L. contributed materials/analysis tools. L.Z. and Q.L. wrote the manuscript, and all authors provided revisions to the manuscript.

Competing interests

The authors declare no competing interests.

Additional information

Supplementary information The online version contains supplementary material available at https://doi.org/10.1038/s41597-024-04058-6.

Correspondence and requests for materials should be addressed to D.W. or Q.L.